Pergamon

Bioorganic & Medicinal Chemistry 7 (1999) 1089–1096

BIOORGANIC & MEDICINAL CHEMISTRY

Inhibition of HIV-1 Tat-TAR Interaction By Diphenylfuran Derivatives: Effects of the Terminal Basic Side Chains

Nathalie Gelus,[a] Christian Bailly,[a,*] François Hamy,[b] Thomas Klimkait,[c] W. David Wilson[d] and David W. Boykin[d]

[a]*INSERM Unité 524 et Laboratoire de Pharmacologie Antitumorale du Centre Oscar Lambret, Place de Verdun, 59045 Lille, France*
[b]*Pharma Research, Novartis Pharma Inc., 4002 Basel, Switzerland*
[c]*Department of Molecular Diagnostics, Institut für Medizinische Mikrobiologie der Universität Basel, Petersplatz 10, CH-4003 Basel, Switzerland*
[d]*Department of Chemistry, Georgia State University, Atlanta, GA 30303, USA*

Received 16 September 1998; accepted 3 November 1998

Abstract—A series of four biscationic diphenylfuran derivatives was used to investigate drug binding to the transactivation response element (TAR) RNA. The drugs, which are active against the *Pneumocystis carinii* pathogen (PCP), differ by the nature of the terminal basic side chains. Furimidazoline (DB60) is more potent at inhibiting binding of the Tat protein to TAR than furamidine (DB75) and the amidine-substituted analogues DB244 and DB226. In vivo studies using the fusion-induced gene stimulation (FIGS) assay entirely agree with the in vitro gel mobility shift data. The capacity of the drugs to antagonize Tat binding correlates with their RNA binding properties determined by melting temperature and RNase protection experiments. Footprinting studies indicate that the bulge region of TAR provides the identity element for the diphenylfurans. Access of the drugs to the major groove cavity at the pyrimidine bulge depends on the bulk of the alkylamine substituents. Experiments using TAR mutants show that the bulge of TAR is critical for drug binding but also reveal that the fit of the drugs into the major groove cavity of TAR does not involve specific contacts with the highly conserved residue U23 or the C·G26-39 base pair. The binding essentially involves shape recognition. The results are also discussed with respect to the known activity of the drug against PCP which is the major cause of mortality in AIDS patients. This study provides guidelines for future development of TAR-targeted anti-HIV-1 drugs.

Introduction

One of the most common causes of mortality in AIDS patients is the *Pneumocystis carinii* pathogen (PCP). The bis(phenylamidinium) derivative pentamidine is active against PCP but its clinical use is restricted due to toxicity and limited oral activity. In recent years, a large number of novel anti-PCP agents have been synthesized. These include aromatic dicationic compounds related to pentamidine[1] and amidino 2,5-diphenylfurans. Furamidine (2,5-bis(4-amidinophenyl)furan, DB75 in Fig. 1) is effective in vivo at submicromolar dosage against *P. carinii* in the immunosuppressed rat model[2] and more potent analogues have been developed recently.[3] There is considerable evidence that interactions with the genome of the pathogen contribute to the pharmacological effects of diphenylfuran derivatives. Most compounds in the series behave as typical DNA minor groove binders and interact selectively with AT-rich sequences.[4] Inhibition of the *Pneumocystis* topoisomerase II enzyme may also contribute to the biological activity.[5,6] Correlations between anti-PCP effects and binding to DNA or DNA-binding proteins have been evidenced.[4]

In addition to interacting with DNA, diphenylfurans can also bind to RNA. Furamidine (DB75) stabilizes the synthetic RNA polymer poly(A)·poly(U). The effect is much more pronounced with furimidazoline (DB60) which forms intercalation complexes with poly(A)·poly(U).[7] Recently we showed that furimidazoline, but not furamidine, can also intercalate at GC sites in DNA.[8]

Because of the potential use of diphenylfurans as anti-PCP agents for the treatment of HIV-infected patients, it is important to determine the factors which govern the interaction of the drugs with DNA versus RNA. Specific interaction with the DNA genome of

Key words: TAR RNA; HIV-1; diphenylfuran; Tat protein; RNA recognition.
*Corresponding author. Tel.: +33-320-16-92-18; fax: +33-320-16-92-29; e-mail: bailly@lille.inserm.fr
Abbreviations: PCP, *Pneumocystis carinii* pathogen; FIGS, fusion-induced gene stimulation.

0968-0896/99/$ - see front matter
PII: S0968-0896(99)00041-3

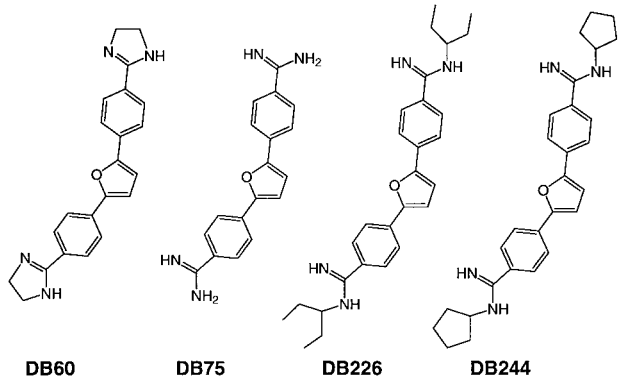

Figure 1. Structure of furimidazoline (DB60), furamidine (DB75) and the two alkyl-substituted amidines DB226 and DB244. These furan derivatives are dications under the conditions of our experiments ($pK_a > 11$).

Pneumocystis is expected for anti-PCP activity whereas interaction with the RNA genome of HIV-1 may produce antiviral effects. Compounds with the ability to target RNA structures essential for the replication of the HIV-1, such as the RRE- and TAR-RNAs, have potential for development as antiviral agents.[9,10] Recently, it was shown that diphenylfurans can interact with the RRE RNA and block binding of the Rev regulatory protein.[11–13] The central aromatic core of the molecule, i.e. the diphenylfuran portion is essential to selectively interact with a bulge region within the RRE RNA but the terminal alkylamine chains also play a significant role.[11,12] To delineate more precisely the role of the cationic side chains of diphenylfurans, we have investigated the binding of four diphenylfurans (Fig. 1) to a small structured RNA from HIV-1. Furamidine (DB75), furimidazoline (DB60) and two analogues with the amidine chains substituted with isopentyl (DB226) or cyclopentyl (DB244) groups were tested. The 59nt TAR RNA which adopts a hairpin structure with a 3-nt bulge located 4 base pairs below the loop was used as a substrate (Fig. 2).[14] The bulge and the surrounding stem region provide the main binding site for the Tat protein and Tat-related basic peptides as well as for antibiotics (e.g. neomycin) and drugs.[15–20] The results indicate that the interaction of the four compounds with the TAR RNA and the inhibition of Tat/TAR-RNA complex formation vary significantly depending on the structure of the terminal side chains. The capacity of the drugs to interact with RNA versus DNA is discussed.

Results

Inhibition of Tat/TAR interaction in vitro

We determined the ability of the diphenylfuran derivatives to inhibit binding of the Tat protein to the stem-loop TAR RNA in a mobility shift assay. In the presence of 20 nM recombinant Tat protein and about 15 nM TAR, the labelled transcript was 40–60% shifted. A single protein–RNA complex is resolved. The capacity of the drugs to interfere with Tat binding depends on the nature of the terminal diamidine side chains. As shown in Figure 3, at a concentration of 10 μM compound DB226 has relatively little effect on Tat binding whereas DB60 completely inhibits protein binding to the RNA substrate. DB75 and DB244 are more efficient than DB226 but not as potent as DB60. The drug concentrations required to cause 50%-dissociation of the Tat-TAR complex (IC_{50}) were determined from the

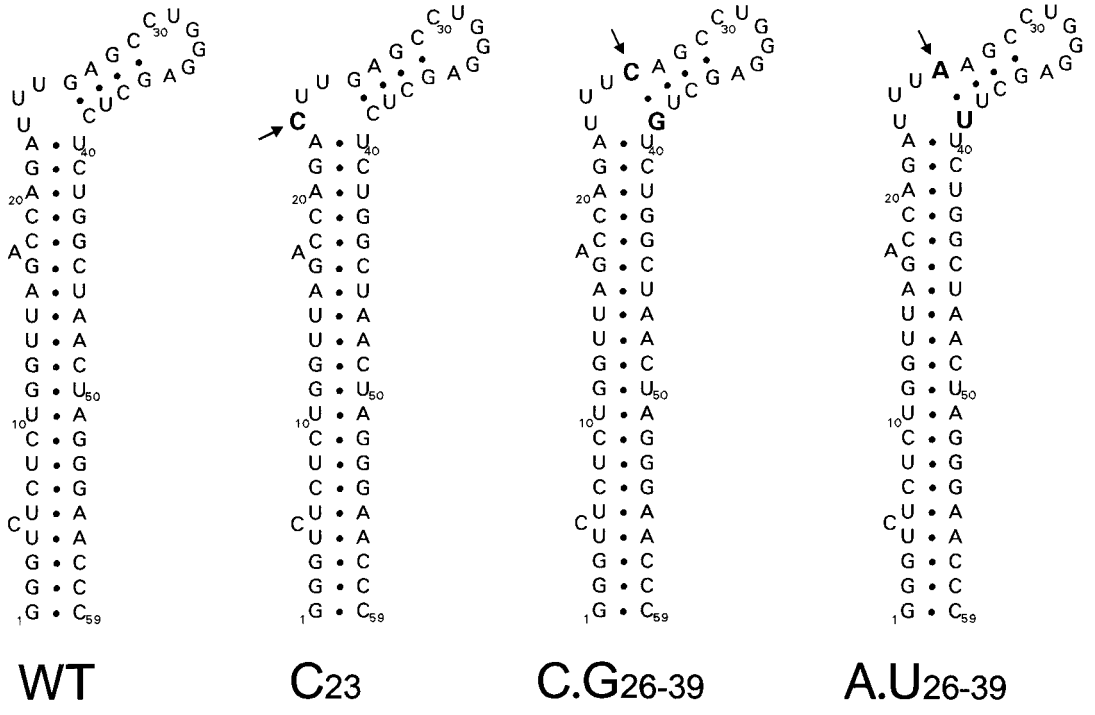

Figure 2. Sequence and secondary structure of the wild type (WT) TAR RNA and the mutants used in this study.

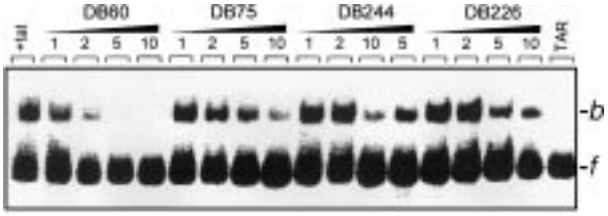

Figure 3. Electrophoretic mobility shift analysis for the inhibition of Tat/TAR complex formation by the diphenylfuran derivatives. The drug concentration (μM) is indicated at the top of each gel lane. Protein–TAR complexes and free RNA are identified as *b* and *f*, respectively. Complexes were separated from unbound RNA by electrophoresis in non-denaturing 8% polyacrylamide gels containing 0.1% Triton X-100.

densitometric analysis of the gel shown in Figure 3 and two other gels (not shown). IC_{50} values of 1, 5, 7 and 12 μM were calculated for compounds DB60, DB75, DB244 and DB226, respectively. The fact that DB60 is over 10 times more potent than DB226 indicates that protein binding inhibition is selective and sensitive to the nature of the furan cationic groups.

FIGS assay

The fusion-induced gene stimulation (FIGS) assay[21,22] was used to determine whether the inhibition of Tat-TAR complex formation observed in vitro translates into inhibition of Tat-mediated transactivation in cells. In this assay, Tat protein constitutively expressed in chronically-infected Hut/4-3 HIV-1 donor cells, is rapidly transferred into an LTR reporter cell via HIV-mediated membrane fusion during cellular coculture. Within hours, Tat can induce β-galactosidase activity from an endogenous recombinant reporter gene. The reporter enzyme is used to localize activated cells utilizing the strict cell association of the blue X-gal conversion product. In addition, the extent of inhibition of Tat-mediated transactivation can be quantitated in the extracellular buffer by a β-galactosidase-dependent conversion of diffusible ortho-nitro-phenyl-galacto (ONPG) to ortho-nitro-phenyl (ONP) and subsequent reading of the optical density at 405 nm.

SX22-1 cells were seeded into 24-well or 96-well plates at densities of 3×10^5 and 2×10^4 cell per well, respectively. Stocks of 10-fold concentrated compounds were dissolved in H_2O and added to the cells at the final concentrations as indicated. On the following day, these pretreated cells were cocultered by adding 1×10^5 (for 24-well) or 1×10^4 (for 96-well) Hut/4-3 HIV-1 donor cells. The next day, cultures were fixed and assayed as described. As shown in Figure 4 where the Tat-inhibitory activity is plotted as a function of compound concentration, DB244 had no effect on Tat-mediated LTR transactivation up to the highest tested compound concentration of 30 μM. DB75 had a mild effect on transactivation with an IC_{50} of about 30 μM. Only DB60 showed a potent inhibition at subtoxic concentrations. DB60 concentrations at and exceeding 10 μM lead to a clear cytostatic/cytotoxic effect, evidenced by significantly reduced cell counts at the time of readout (not

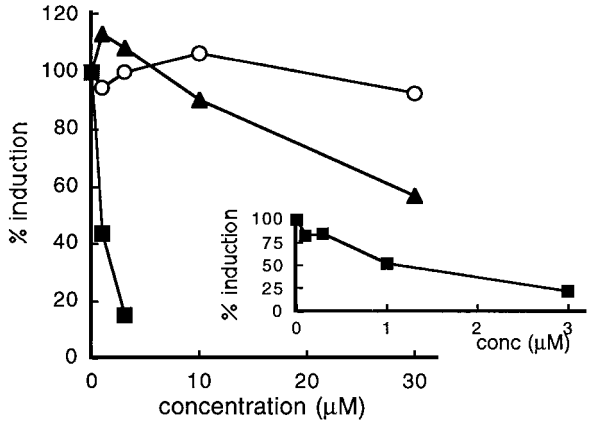

Figure 4. Quantification of ONPG reading in the β-Gal-driven ONPG conversion (expressed as percent induction compared to untreated control) as a function of the drug concentration. (■) DB60, (▲) DB75 and (○) DB244. Inset shows the activity of DB60 at lower concentrations.

shown). At ≤3 μM there was no apparent effect on cell proliferation rates. Further compound titration revealed an IC_{50} for DB60 of about 1 μM (inset in Fig. 4).

Drug-TAR RNA interaction

We examined the ability of the diphenylfuran derivatives to alter the thermal denaturation profile of the TAR RNA. Representative melting curves for the free RNA and its complexes with the test drugs are shown in Figure 5. The helix-to-coil transition occurs at 54 °C in the absence of drugs. The *T*m is shifted to higher temperature with all four drugs but the extent of stabilization varies significantly from one analogue to another. Δ*T*m values (*T*m complex–*T*m RNA) of 8–10 °C were measured with DB226 and DB244. Much larger Δ*T*m were measured with the two other drugs, the maximum effect being obtained with DB60 with a Δ*T*m of 24 °C. The *T*m results indicate that DB60 exhibits the highest affinity for TAR. There is a good correlation between the *T*m measurements and the results of the gel shift assays. In both cases, the drugs rank in the order DB60 > DB75 > DB244 > DB226.

Sequence-selective binding

The drug binding site on the TAR RNA was identified by footprinting using RNase A as a cleaving agent. This

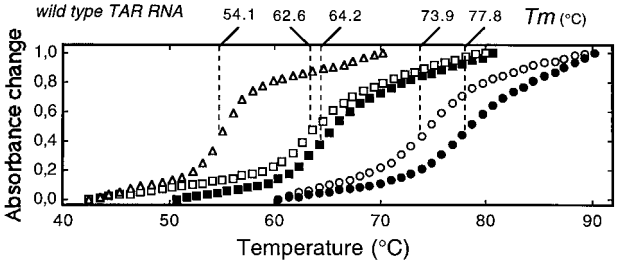

Figure 5. Thermal denaturation curves for the wild-type TAR in the absence (△) and presence of DB226 (□), DB244 (■), DB75 (○) and DB60 (●) (5 μM each). The indicated *T*m values (in °C) were obtained from first-derivative plots.

enzyme preferentially cuts at the loop (C29–U31) and opposite the bulge (C37–C39) rather than the two double-stranded stem regions of the RNA. The pyrimidine bulge (U23–U25) is also poorly cut. The gel in Figure 6 shows the cleavage patterns obtained with the wild type TAR in the absence and presence of the four diphenylfuran derivatives. With DB60 and DB75, and to a lesser extent with DB244, the strong cleavage located opposite to the pyrimidine bulge (positions 36–40) is largely reduced in the presence of the drug. There is no such effect with DB226. The same results were obtained using the V1 ribonuclease (not shown). At concentrations $< 10\,\mu M$ the cutting rate at the loop region (around positions 30–35) is not significantly affected but at concentrations $\geq 25\,\mu M$ the cleavage at C29-U31 becomes slightly reduced suggesting that a second molecule perhaps binds to the apical loop under these conditions.

RNase A is detecting specific binding of DB60, DB75 and DB244 to the GCUCU site (positions 36–40). The extent of protection at this site is proportional to the drug concentration. The footprinting results are entirely consistent with the gel mobility shift data. DB60 which is the best Tat-antagonist of the four derivatives, produces the strongest footprints. In contrast, DB226 which is a weak inhibitor of Tat binding, fails to inhibit RNase A cleavage. From the footprinting data we can conclude that the inhibition of Tat binding arises from direct interaction between the drug and the bulge region of TAR.

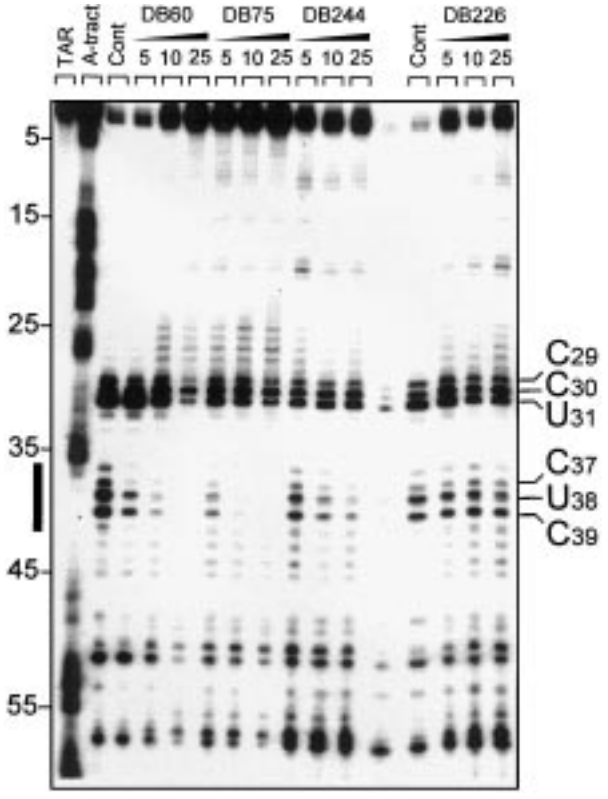

Figure 6. RNase A footprinting of the diphenylfuran derivatives on wild-type TAR. The RNA was 3′-end labelled with [^{32}P]cytidine biphosphate and T4 RNA ligase. The cleavage products of RNAase digestion were resolved on a 10% polyacrylamide gel containing 8 M urea. The concentration (μM) of the drug is shown at the top of the appropriate gel lanes. Control tracks labelled "Cont" contained no drug. Track labelled A represents diethylpyrocarbonate-aniline markers specific for adenines. Lane marked "RNA" contain the [^{32}P]-labelled RNA alone, incubated without drug or enzyme; this sample serves as a control to assess background nicking of the RNA preparation. Vertical black bars refer to the position of the binding site.

We interpret the base protection effects as being due to direct interaction with the ligand but in fact we do not exclude the possibility that the protection arises from drug-induced structural changes. Protection caused by drug-dependent conformational changes that results in formation of a RNase A-resistant local structure cannot be readily distinguished from those caused by direct ligand–RNA contacts. To address this issue, we probed the TAR structure with the bleomycin·Fe^{II} complex. In addition to being a potent DNA cleaving agent, the antitumor drug bleomycin functions as a RNA cleaver and can be used as a probe of RNA conformation.[23–25] We examined the effect of the diphenylfuran derivatives on the cleavage of TAR by the bleomycin·Fe^{II} complex. This is the first time this cleaving agent is used to probe drug-induced conformational changes of the TAR RNA. As shown in Figure 7, in the absence of a ligand, attack of the TAR RNA by the bleomycin·Fe^{II} complex only produced discrete cleavage sites at C30, C57 and a weaker cleavage at G53. The same cutting sites were detected in the presence of DB75 and DB60 (20 μM each) suggesting that these two drugs do not markedly change the structure of the RNA. In sharp contrast, the bleomycin-induced cleavage profile was markedly changed in the presence of actinomycin, a well known DNA-intercalating antitumor antibiotic. In the presence of 10 μM actinomycin, the entire loop becomes accessible for bleomycin cleavage. Strong cutting can be detected at the CUGG site (positions 30–33). Unlike what was observed with the diphenylfuran derivatives, the conformational changes produced by actinomycin enhanced the RNA-degradative activity of bleomycin A2. Therefore, we can confidently consider that the footprint at the pyrimidine bulge region of TAR obtained with DB60 and its analogues arises from a direct drug–RNA interaction.

Drug binding to TAR mutants

The observation that DB60 and analogues bind selectively to the bulge region of TAR prompted us to investigate further the recognition process with TAR mutants having modified bulge sequences. We used two TAR mutants for which the G·26–39 pair is either reverted to a C·G pair or replaced with an A·U pair (Fig. 2). The G·C26–39 pair is crucial for Tat binding.[26] A mutant having the U23 residue replaced with a C residue was also prepared so as to determine the role of this highly conserved uridine residue which is known to be critical for binding of the Tat protein.[27] In addition, we used a bulge-free mutant with a deletion of the UUU triplet at positions 23–25. The interaction of the diphenylfuran derivatives with these 60 nucleotides long RNA (all synthesized by in vitro transcription) was studied by RNase A footprinting and melting temperature experiments.

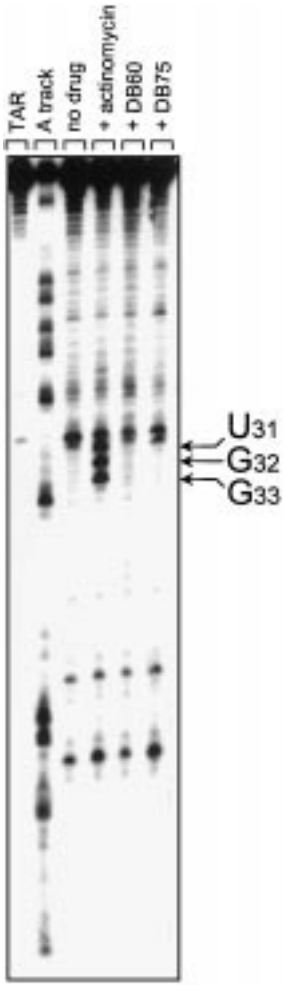

Figure 7. Cleavage of the TAR RNA by the Fe^{II} complex of bleomycin A2 (500 μM) in the absence and presence of actinomycin (10 μM) or the diphenylfuran derivatives DB75 and DB60 (20 μM each). Actinomycin-induced cleavage sites are pointed out by the arrows. Other details as for Figure 6.

*T*m of 54.1, 54.3, 51.3 and 53.3 °C were determined for WT, C·G26–39, A·U26–39 and C23 TAR, respectively (average of three independent measurements). In the presence of DB60, the *T*m values increase considerably and the Δ*T*m values reached 23–27 °C, be it with the wild type (WT) or the mutants RNA. With the three other compounds, DB75, DB226 and DB244, the Δ*T*m values were lower but again we detected no significant variation using WT TAR or the mutants (Fig. 8). It is only with the bulge-free analogue that the Δ*T*m values fall significantly. For example, the Δ*T*m amounts to 24 °C with WT TAR and to 4 °C with ΔU-TAR in the presence of DB60. We conclude that the bulge region of TAR is essential for optimal drug binding but neither the U23 residue nor the G·C26–39 play a direct role in the binding reaction.

RNase protection experiments with the TAR mutants provided the same results as with WT TAR. Typical RNase A footprinting gels obtained with C·G26–39 TAR and C23 TAR are presented in Figure 9. A clear footprint at the GCUCU site can be seen with DB60

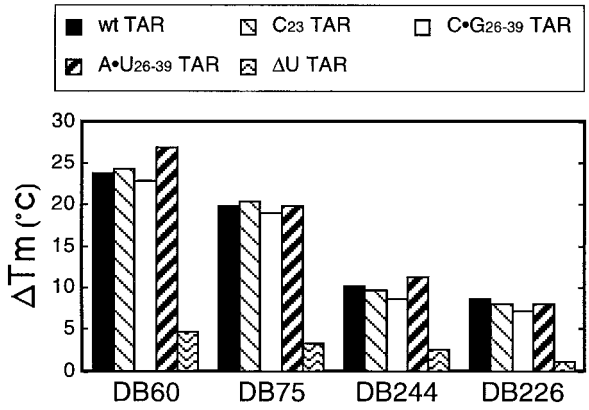

Figure 8. Δ*T*m values measured with the diphenylfuran derivatives with the wild-type TAR RNA and the mutants.

and DB75, just as observed with WT TAR. Neither the replacement of the G·C26–39 pair with a C·G pair nor the U→C23 substitution hinder drug binding. ΔU-TAR could not be used for the footprinting experiments. Indeed, because of the removal of the bulge, the double-stranded sequence at position 36–40 was now cut only poorly by RNase A and therefore it was not possible to monitor potential drug binding to this sequence.

Discussion

The effects of the drugs on Tat binding were monitored both in vitro and in cells. It is remarkable that the results of the shift assay quantitatively agree quite well with those of the FIGS assay. At a concentration of 1 μM, furimidazoline (DB60) reduces Tat binding to TAR by 50% in vitro and a roughly equivalent concentration of DB60 is needed to inhibit Tat-mediated transactivation in HIV-infected cells. In contrast, DB226 and DB244 which poorly inhibit Tat binding in vitro, have no effect on transactivation. The intermediate TAR binder DB75 shows a proportional effect on transactivation. On the one hand, the results suggest that the TAR RNA represents a promising target for DB60 in cells. On the other hand, the study shows that the spatial presentation of the terminal basic side chains is determinant for optimal activity. The results of the present study concur with those obtained with the RRE that diphenylfuran derivatives bearing bulky alkylamine substituents (e.g. dimethylaminopropyl, cyclopentyl) have restricted access to the groove of the A-form RNA. Shorter molecules, such as DB75 and DB60, fits more easily into the cavity created by the pyrimidine bulge.

We considered that the G·C26–39 base pair and/or the U23 base located at the bulge region of TAR would have a major influence on drug binding for two reasons. First, these base residues are essential for Tat binding: the highly conserved U23 residue comes close to argininamide and G26 makes interaction with argininamide[27] and the mutation of the G·C26–39 base pair considerably reduces Tat binding.[28] Second, we have recently shown that the G·C26–39 base pair is the main

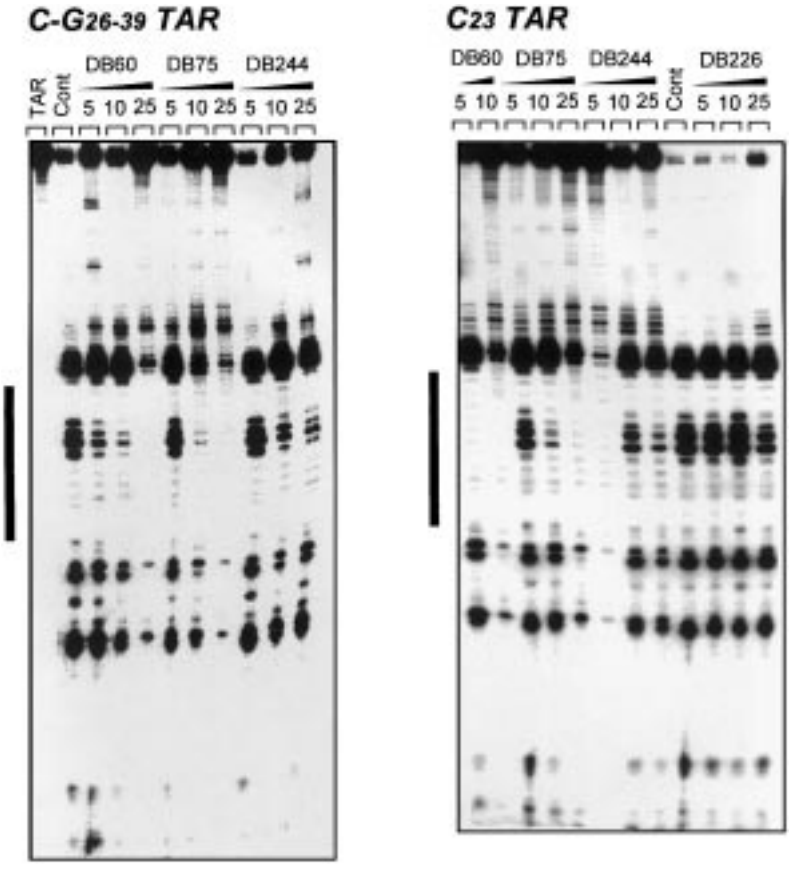

Figure 9. RNase A footprinting of the diphenylfuran derivatives on C·G26–39 and C23 TAR. Other details as for Figure 6.

molecular determinant for tight binding of an acridine-based Tat antagonist to TAR.[29] We therefore anticipated that the binding activity of the diphenylfuran derivatives would also be sensitive to the modifications of these base residues. The bulge region of TAR plays an important role in the interaction of diphenylfurans with the RNA (as judged from the *T*m and footprinting experiments) but neither substitution at the U23 residue, nor mutation at the G·C26–39 base pair perturb the binding of the drugs to the RNA. We conclude that the fit of furamidine into the major groove cavity of TAR does not involve specific contacts with these residues but involve shape recognition. The drug may engage in contacts with other residue, e.g. the A·U27–38 base pair which is also highly conserved and important for Tat binding.[26] Alternatively, the drug–RNA interaction is perhaps mainly based on the sequence-dependent deformability of the RNA target site rather than on the chemical complementarity between the ligand and the RNA bases (analogue readout as opposed to base-specific digital readout). The interaction of the flexible Tat protein with TAR also depends strongly upon the tertiary structure of the binding pocket within TAR.[30] The fact that furamidine binds quite well to both the bulge of the RRE and TAR RNA suggests that the ligand recognizes the global structure/conformation of the RNA bulge rather than a primary base sequence. More detailed proposals will have to await the results of further experiments using diverse techniques such as NMR.

As mentioned in the introduction, diphenylfuran derivatives exhibit potent anti-PCP activities, presumably as a result of their interaction with the DNA genome of the pathogen.[2–4] In this case, the drug–DNA interaction involves contacts into the minor groove of AT-rich sequences. However, binding to GC-rich sequences can also occur under certain circumstances. We have recently shown that furimidazoline (DB60) form intercalation complexes with GC-containing DNA sequences.[8] Both DB60 and DB75 bind to AT-rich DNA sequences but only DB60 can intercalate at GC-rich sequences. In DNase I footprinting experiments, practically no specific binding to AT-containing sites was seen with DB60 whereas the three analogues DB75, DB226 and DB244 protect AT sequences from cutting by DNase I.[32] As a result, furimidazoline is less active against PCP than its congeners. In terms of anti-PCP activity, the compounds rank in the order DB244 > DB75 ≫ DB226 > DB60.[23] Apparently, there is a correlation between the high propensity of compound DB60 to intercalate into GC-rich DNA sequences and its ability to bind to TAR and RRE RNA.

Experimental

Chemicals

The synthesis of the drugs has been reported.[23] All other chemicals were analytical grade reagents, and solutions

were prepared with doubly distilled sterile water to prevent from nuclease contamination. Tubes and tips were treated with 1% diethylpyrocarbonate (DEPC from Sigma).

In vitro transcription

Synthetic oligonucleotides corresponding to the wild-type or mutated TAR sequences were cloned between *Hin*dIII and *Eco*RI sites of the pUC19 plasmid. After digestion with *Eco*RI, the RNA was transcribed as a run-off product of 60 nucleotides from the T3 RNA polymerase promoter. In each case the transcript included an additional G residue on the 3′-end derived from the *Eco*RI cleavage site. Transcription reaction was performed in buffer containing 40 mM Tris–HCl, pH 7.4, 25 mM NaCl, 16 mM MgCl2, 10 mM DTT and 1 mM NTPs. The reaction was initiated by addition of 10 μg linearized plasmid DNA template and 40 units T3 RNA polymerase and incubated for 2 h at 37 °C. Nucleic acids were then fractionated on a 10% (w/v) polyacrylamide gel containing 8 M urea in TBE buffer (89 mM tris-borate pH 8.3, 10 mM EDTA). After electrophoresis, the RNA was eluted in water for 18 h at 4 °C and precipitated with ethanol. The RNA was resuspended in water to give a 500 μM stock solution (ε^{260}/phosphate = 10688 $M^{-1} \times cm^{-1}$). For the footprinting experiments, the RNA was 3′-end labelled with [^{32}P]cytidine biphosphate and T4 RNA ligase and then repurified from a 10% denaturing acrylamide gel.

Gel mobility shift assay

Recombinant Tat protein was prepared as described.[19] Binding reaction (20 μL) contained the ^{32}P-labeled TAR RNA (2 μL, about 15 nM), 20 nM recombinant Tat protein and varying concentration of the test compound in a TK buffer consisting of 50 mM Tris–HCl (pH 7.4), 20 mM KCl, 5 mM DTT and 0.1% Triton X-100. Samples were incubated for 30 min at 4 °C prior to electrophoresis on a 8% nondenaturing polyacrylamide gel. After about 1.5 h electrophoresis at 200 V and at 4 °C, the gel was dried and analyzed on a Phosphor-imager (Molecular Dynamics).

Melting temperature studies

Absorption spectra were recorded on a Uvikon 943 spectrophotometer. The 12-cells holder was thermostated with a Neslab RTE 111 cryostat. Drug–RNA complexes were prepared by adding aliquots of a concentrated drug solution to a RNA solution at constant concentration (usually 20 μM) in BPE buffer pH 7.1 (6 mM Na_2HPO_4, 2 mM $Na_2H_2PO_4$, 1 mM EDTA). A heating rate of 1 °C/min was used and data points were collected every 30 s. The temperature inside the cuvette was monitored by using a thermocouple. The absorbance at 260 nm was measured over the range 25–90 °C in 1 cm path length reduced volume quartz cells. The ''melting'' temperature *T*m was taken as the mid-point of the hyperchromic transition determined from first derivatives plots. The reproducibility of the *T*m measurements was ± 1 °C.

RNase A footprinting, gel electrophoresis and data processing

The procedure for the footprinting experiments has been described previously.[31] Briefly, samples of the labelled RNA fragment were incubated with a buffered solution containing the desired drug concentration. After 20 min incubation at 4 °C to ensure equilibration, the digestion was initiated by addition of the RNase A solution. After 1 min incubation at room temperature, the reaction was stopped by freeze drying and samples were lyophilized. The RNA in each tube was resuspended in 5 μL of formamide-TBE loading buffer, denatured at 90 °C for 4 min then chilled in ice for 4 min prior to loading on to a 0.3 mm thick, 10% polyacrylamide gel containing 8 M urea and TBE buffer (89 mM Tris base, 89 mM boric acid, 2.5 mM Na_2 EDTA, pH 8.3). After 2 h electrophoresis at 1500 V, the gel was soaked in 10% acetic acid for 10 min, transferred to Whatman 3 MM paper, dried under vacuum at 80 °C and then analyzed on the Phosphorimager (Molecular Dynamics). Each resolved band on the autoradiograph was assigned to a particular bond within the RNA fragment by comparison of its position relative to sequencing standards generated by treatment of the RNA with diethylpyrocarbonate followed by aniline-induced cleavage at the modified bases (A track).

Cellular trans-activation assay

'FIGS-assays' were performed as described.[19] Briefly, the HeLaT4-derived reporter cell line SX 22-1 was cocultivated with Hut/4-3 lymphocytes at a ratio of 3:1. The latter cells constitutively generate infectious virus particles. Cocultivation of the SX 22-1 reporter cells with the HIV-1 donor Hut/4-3 results in rapid cell fusion within hours. Thereby Tat protein from the HIV-1 donor enters the reporter cells and induces the endogenous HIV LTR lacZ gene present in the SX22-1 cells. After overnight cocultivation the cultures were fixed. Cells were stained for β-galactosidase activity using X-gal as a substrate. For photometric quantification the fixed cultures were subsequently incubated with ortho-nitro-phenyl-galactopyranoside (ONPG) as β-galactosidase substrate, which is enzymatically converted to the chromophoric ortho-nitrophenol (ONP) and absorption measured at 405 nm.

Transfection FIGS

Alternatively, seeded SX22-1 cells were transfected with plasmid DNA of the complete, infectious HIV-1 clone pNL4-3 on the day after compound addition. Amounts of 0.6 μg for 24-wells and 0.2 μg for 96-wells were transfected using the Fugene protocol (Boehringer-Mannheim, GER). Two days after transfection cells were fixed and assayed.

Cell culture

Cell media, media supplements, PBS-buffer, HEPES, and sera were purchased from Life Technologies (Paisley, UK). SX22-1 cells were cultured in DMEM

with 4500 mg/mL glucose, 10% fetal bovine serum (FBS), supplemented with Penicillin (500 IU/mL)/Streptomycin (500 μg/mL). Confluent cultures were trypsinized and passaged 1:20. Hut/4-3 cells were maintained in RPMI, 10% FBS, supplemented with Penicillin/Streptomycin and 10 mM HEPES. Cells were kept at densities between 2×10^5 and 3×10^6.

Acknowledgements

This work was done under the support of research grants (to C.B.) from the Agence Nationale de la Recherche sur le SIDA (ANRS); (to W.D.W and D.W.B.) from NIH grant NIAID AI-33363 and the Georgia Research Alliance.

References and Notes

1. Hall, J. E.; Kerrigan, J. E.; Ramachadran, K.; Bender, B. C.; Stanko, J. P.; Jones, S. K.; Patrick, D. A.; Tidwell, R. R. *Agents Chemother*. **1998**, *42*, 666.
2. Boykin, D. W.; Kumar, A.; Spychala, J.; Zhou, M.; Lombardi, R. L.; Wilson, W. D.; Dykstra, C. C.; Jones, S. K.; Hall, J. E.; Tidwell, R. R.; Laughton, C.; Nunn, C. M.; Neidle, S. *J. Med. Chem*. **1995**, *38*, 912.
3. Boykin, D. W.; Kumar, A.; Xiao, G.; Wilson, W. D.; Bender, B. C.; McCurdy, D. R.; Hall, J. E.; Tidwell, R. R. *J. Med. Chem*. **1998**, *41*, 124.
4. Trent, J. O.; Clark, G. R.; Kumar, A.; Wilson, W. D.; Boykin, D. W.; Hall, J. E.; Tidwell, R. R.; Blagburn, B. L.; Neidle, S. *J. Med. Chem*. **1996**, *39*, 4554.
5. Dykstra, C. C.; Tidwell, R. R. *J. Protozool*. **1991**, *38*, 78S.
6. Dykstra, C. C.; McClernon, D. R.; Elwell, L. P.; Tidwell, R. R. *Agents Chemother*. **1994**, *38*, 1890.
7. Zhao, M.; Ratmeyer, L.; Peloquin, R. G.; Yao, S.; Kumar, A.; Spychala, J.; Boykin, D. W.; Wilson, W. D. *Bioorg. Med. Chem*. **1995**, *3*, 785.
8. Wilson, W. D.; Tanious, F. A.; Ding, D.; Kumar, A.; Boykin, D. W.; Colson, P.; Houssier, C.; Bailly, C. *J. Am. Chem. Soc*. **1998**, *120*, 10310.
9. Pearson, N. D.; Prescott, C. D. *Chem. Biol*. **1997**, *4*, 409.
10. Chow, C. S.; Bogdan, F. M. *Chem. Rev*. **1997**, *97,* 1489.
11. Zapp, M. L.; Young, D. W.; Kumar, A.; Singh, R.; Boykin, D. W.; Wilson, W. D.; Green, M. R. *Bioorg. Med. Chem*. **1997**, *5*, 1149.
12. Ratmeyer, L.; Zapp, M. L.; Green, M. R.; Vinayak, R.; Kumar, A.; Boykin, D. W.; Wilson, W. D. *Biochemistry* **1996**, *35*, 13689.
13. Li, K.; Fernandez-Saiz, M.; Rigl, C. T.; Kumar, A.; Ragunathan, K. G.; McConnaughie, A. W.; Boykin, D. W.; Schneider, H.-J.; Wilson, W. D. *Bioorg. Med. Chem*. **1997**, *5*, 1157.
14. Jones, K. A.; Peterlin, B. M. *Annu. Rev. Biochem*. **1994**, *63*, 717.
15. Mei, H.-Y.; Galan, A. A.; Halim, N. S.; Mack, D. P.; Moreland, D. W.; Sanders, K. B.; Truong, H.N.; Czarnik, A. W. *Bioorg. Med. Chem. Lett*. **1995**, *5*, 2755.
16. Mei, H.-Y., Mack, D.P., Galan, A.A., Halim, N.S., Heldsinger, A., Loo, J.A., Moreland, D.W., Sannes-Lowery, K. A.; Sharmeen, L.; Truong, H. N.; Czarnik, A. W. *Bioorg. Med. Chem*. **1997**, *5*, 1173.
17. Wang, S.; Huber, P. W.; Cui, M.; Czarnik, A. W.; Mei, H.-Y. *Biochemistry* **1998**, *37*, 5549.
18. Hamy, F.; Felder, E. R.; Heizmann, G.; Lazdins, J.; Aboul-ela, F.; Varani, G.; Karn, J.; Klimkait, T. *Proc. Natl. Acad. Sci. USA* **1997**, *94*, 3548.
19. Hamy, F.; Brondani, V.; Flörsheimer, A.; Stark, W.; Blommers, M. J.; Klimkait, T. *Biochemistry* **1998**, *37*, 5086.
20. Mei, H.-Y.; Cui, M.; Heldsinger, A.; Lemrow, S. M.; Loo, J. A.; Sannes-Lowery, K. A.; Sharmeen, L.; Czarnik, A. W. *Biochemistry* **1998**, *37*, 14204.
21. Wyatt, J. R.; Vickers, T. A.; Roberson, J. L.; Buckheit, R. W. J.; Klimkait, T.; DeBaets, E.; Davis, P. W.; Rayner, B.; Imbach, J. L.; Ecker, D. J. *Proc. Natl. Acad. Sci. USA* **1994**, *91*, 1356.
22. Klimkait, T.; Stauffer, F.; Lupo, E.; Sonderegger-Rubli, C. *Arch. Virol*. **1998**, *143*, 1.
23. Hecht, S. M. *Bioconjugate Chem*. **1994**, *5*, 513.
24. Holmes, C. E.; Carter, B. J.; Hecht, S. M. *Biochemistry* **1993**, *32*, 4293.
25. Holmes, C. E.; Abraham, A. T.; Hecht, S. M.; Florentz, C.; Giegé, R. *Nucleic Acids Res*. **1996**, *24*, 3399.
26. Churcher, M. J.; Lamont, C.; Hamy, F.; Dingwall, C.; Green, S. M.; Lowe, A. D.; Butler, P. J. G.; Gait, M. J.; Karn, J. *J. Mol. Biol*. **1993**, *230*, 90.
27. Gait, M. J.; Karn, J. *Trends Biochem. Sci*. **1993**, *18*, 255.
28. Aboul-ela, F.; Karn, J.; Varani, G. *J. Mol. Biol*. **1995**, *253*, 313.
29. Gelus, N.; Hamy, F.; Bailly, C. *Bioorg. Med. Chem*. **1999**, *7*, 1079.
30. Garbesi, A.; Hamy, F.; Maffini, M.; Albrecht, G.; Klimkait, T. *Nucleic Acids Res*. **1998**, *26*, 2886.
31. Bailly, C.; Colson, P.; Houssier, C.; Hamy, F. *Nucleic Acids Res*. **1996**, *24*, 1460.
32. Bailly, C.; Dassonneville, L.; Carrasco, C.; Lucas, D.; Kumar, A.; Boykin, D. W.; Wilson, W. D. *Anti-Cancer Drug Design* **1999**, *14*, 47–60.